Theoretical and Applied Climatology
https://doi.org/10.1007/s00704-018-2555-9

ORIGINAL PAPER

Assessment of CALIOP and MODIS aerosol products over Iran to explore air quality

S. Zahedi Asl[1] · A. Farid[2] · Y.-S. Choi[3,4]

Received: 8 October 2016 / Accepted: 28 June 2018

Abstract
Monitoring air quality is crucial for Middle East countries such as Iran, where dust and polluted aerosol sources heavily influence local air quality. The use of active satellite remote sensing techniques is therefore considered in monitoring air quality. This study presents an initial assessment of NASA's Cloud-Aerosol LIdar with Orthogonal Polarization (CALIOP) aerosol data over Tabriz and Mashhad cities in the north-western and north-eastern regions of Iran. We examined the Cloud and Aerosol Discrimination (CAD) score values, extinction coefficient, and the CALIOP Vertical Feature Mask (VFM) data product and Moderate Resolution Imaging Spectroradiometer (MODIS) Deep Blue Aerosol Optical Depth (DBOD) at wavelength of 0.55 μm. The ground-based PM_{10} measurements were analyzed for different time periods, seasons, and years from 2005 to 2016. We investigated the profiles of the particle backscatter and extinction coefficient, as well as information about the determined feature types (e.g., clouds or aerosols) and aerosol subtypes (e.g., dust, and smoke) from the VFM data product in 2 months of August 2009 and July 2013, which were statistically selected from 2009 to 2016. Evaluation of the comparison of the relative humidity, temperature, and their inversion shows that the performance of the CALIOP in the detection of aerosols in mid-troposphere (around 5.0 km) is better than cloud detection. Additionally, the correlations of the PM_{10} concentration, MODIS AOD, and MODIS DBOD were investigated for January 2005 to December 2014. The overall analyses show that monthly ground-based PM_{10} concentration measurements reveal better correlation ($r = 0.65$ and 0.67 for Tabriz and Mashhad, respectively) with monthly MODIS-DBOD than MODIS-AOD for different seasons. The observed differences in the investigation of the CALIPSO dataset with the actual measured values and the overall correlation results show that the cloud and aerosol discrimination algorithm should be modified and calibrated based on local measurements of relative humidity, temperature, and their inversions, MODIS-DBOD, and ground-based PM_{10} for the Iran region.

Keywords CALIPSO · Aerosol · Dust · VFM · MODIS DBOD · MODIS AOD · PM_{10}

1 Introduction

Iran is located in a region that is heavily affected by dust storms (Cao et al. 2015) and has several desert fields, including the Dasht-e Kavir (Great Kavir) and Lut deserts (Laity 2009). The air quality issue is one of the major environmental problems in recent years, due to the intensification of drought, which has affected most parts of the Middle East countries. In addition, according to Liu et al. (2009), specific geographical and political conditions prevailing in the Middle East, and also geographical location in the dust belt pathway, increases the necessity of monitoring and discrimination of clouds and aerosols for this region, especially for Iran. The study area includes western and eastern regions located between (44 and 63)° eastern longitude and (25 and 40)° northern latitude of Iran. Figure 1 depicts the Iran region as a study area in the Middle East.

Satellite remote sensing can be used to monitor the air quality of the areas that are not easily accessible for field measurements (Gupta and Christopher 2008; Yap and Hashim 2013). The Cloud-Aerosol LIdar with Orthogonal Polarization

✉ A. Farid
farid-h@ferdowsi.um.ac.ir

[1] Department of Remote Sensing Engineering, Faculty of Engineering, Ferdowsi University of Mashhad (FUM), Mashhad, Iran

[2] Department of Water Engineering, Faculty of Agriculture, Ferdowsi University of Mashhad (FUM), Mashhad, Iran

[3] Department of Environmental Science and Engineering, Ewha Womans University, Seoul, South Korea

[4] NASA Jet Propulsion Laboratory, Pasadena, CA, USA

Published online: 03 August 2018

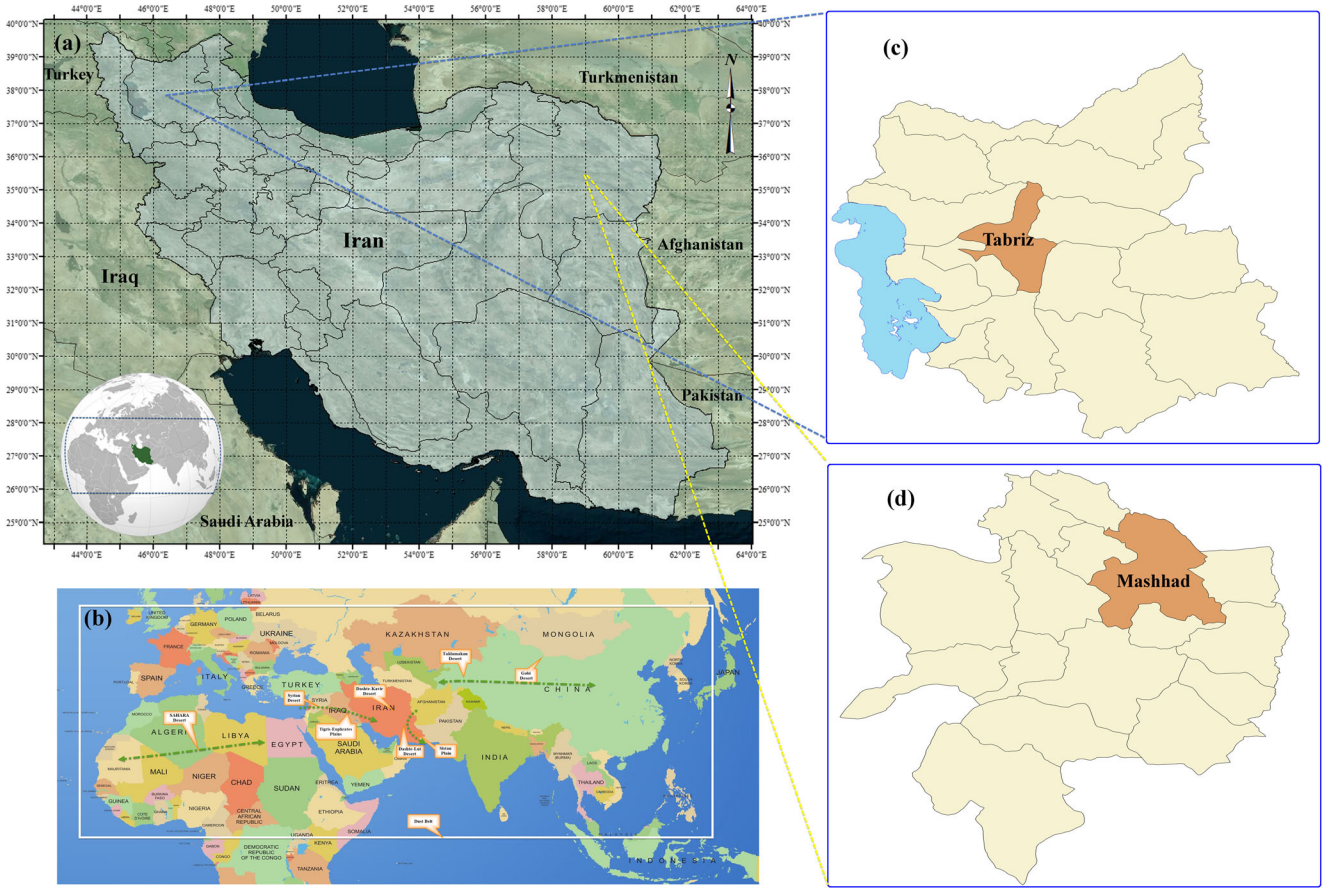

Fig. 1 Maps of the **a** study area in the Middle East and **b** dust belt

(CALIOP) onboard the Cloud-Aerosol Lidar and Infrared Pathfinder Satellite Observations (CALIPSO) satellite is one of the active instruments of NASA's A-Train satellites for monitoring air quality, which provides both daytime and nighttime measurements (Liu et al. 2009). It can obtain a vertically resolved profile of the object under consideration (capable of distinguishing between aerosol and cloud layers, and retrieving their vertical position), and it has high capability for a wide range of scientific studies associated with clouds and aerosols. More importantly, CALIOP can measure aerosol backscatter and infer extinction coefficient profiles in both cloudy and cloud-free situations (Chand et al. 2008; Winker et al. 2010).

Liu et al. (2009) compared the CALIOP dataset with the CloudSat radar dataset on the Gobi desert, and found aerosols at an altitude around 10 km, which, however, CALIOP misclassified as a cloud. Chan and Comiso (2011) used a combination of three sensor datasets (CALIOP, CloudSat, and Moderate Resolution Imaging Spectroradiometer (MODIS)) to provide good complementary information about certain types of clouds, which might be clear in one sensor detection, but not in others and/or mistakenly classified. Considering that CALIOP and CloudSat are designed exclusively to measure the vertical structure of aerosols and clouds from space, unexpectedly, some features are not detected even in high-resolution datasets, but those undetected features are detected in the MODIS dataset. Yu et al. (2012) examined the feasibility of combining Ozone Monitoring Instrument (OMI) aerosol index and MODIS cloud optical depth to derive aerosol properties. Zieger et al. (2011) studied the optical properties and particle physics of aerosol in situ measurements for 4 months in Cabauw, the Netherlands. They demonstrated that ambient aerosol particles experience hygroscopic growth at enhanced Relative Humidity (RH). The microphysical and optical properties of aerosols are also strongly dependent on RH.

Aerosol optical depth (AOD) from the MODIS is a significant indicator of the air quality in describing the aerosol distribution and air pollution studies for either a local or global domain (Duncan et al. 2014; Liu et al. 2007; Mei et al. 2009). Various studies have been carried out with various satellite products, including MODIS Deep Blue (DBOD) and MODIS AOD products, to find the relationship between $PM_{2.5}$ and PM_{10}, and also estimate the concentration of ground-level particulate matters for different regions of the world (Choi et al. 2009; Emili et al. 2010; Escribano et al. 2014; Lee et al. 2016; Lei and Wang 2014; Song et al. 2009; Tian and Chen 2010a, b; Van Donkelaar et al. 2006, 2011; Yap and Hashim 2013). It should be mentioned that the defined models are not universally applicable, due to the low

correlation between PM, AOD, and DBOD. However, for the regional models, the correlation coefficient of $PM_{2.5}$ and PM_{10} with AOD and DBOD varies from (0.4 to 0.9).

Tian and Chen (2010a) used a semi-empirical model to predict the hourly ground-level fine particulate matter ($PM_{2.5}$) concentration based on corrected MODIS AOD with ground and satellite meteorological information, at a regional scale in southern Ontario, Canada for 2004. Overall, the model is able to explain 65% of the variability in ground-level $PM_{2.5}$ concentration. Zheng et al. (2013) used AOD data retrieved from the MODIS to investigate the spatial and temporal variations of PM_{10} pollution in the Pearl River Delta (PRD) region in China for 2006 to 2008. The results show that the estimated PM_{10} concentrations from the regression models appeared to be the highest in winter, and the lowest in summer. Also, a high PM_{10} concentration band was detected over the inner part of the PRD region, where heavy industries and dense populations are located.

The primary purpose of this study is to use the CALIOP satellite data over Iran, where the air is highly polluted, dusty, and dry, despite a lack of field measurements. However, the performance of the CALIPSO satellite over this region has remained untested, and any related analytical and processing issues have yet to be identified. We explored this issue mainly by using the quality flags (the Cloud-Aerosol Discrimination (CAD) threshold or CAD score) that are indicative of the quality of the CALIOP aerosol profile products, MODIS DBOD and AOD at wavelengths of 0.55 μm, and the ground-based PM_{10} measurements. Note that these ground-based PM_{10} measurements are collected from six and seven independent air-quality monitoring stations by the Department of Environment (DOE) of Tabriz and Mashhad, respectively, Iran from 2005 to 2016.

As we will show later, the mean/relative extinction coefficient uncertainty explains why, when interpreting the CALIOP data, it is important to pay attention to the quality flags. The CAD threshold that we selected required aerosols to have CAD scores of less than −20 (Liu et al. 2009). In addition, we derived an example of the aerosol feature and its sub-type classification over some regions of Iran. Based on the Vertical Feature Mask (VFM) data product, it was seen that the classification algorithm has identified some features correctly for this region. Additionally, in order to evaluate the feature layers from the CALIOP data for this region, these layers are compared with field measurement of relative humidity, temperature, and its inversion, which will be explained in Section 3.

2 Data and method

2.1 Description of CALIOP and products

CALIOP is a dual-wavelength ((1064 and 532) nm), polarization-sensitive elastic backscatter lidar in CALIPSO. The transmitted laser beam is linearly polarized, and the two polarization-sensitive 532-nm (parallel and perpendicular) receiver channels measure the linear depolarization degree of the returned signal (Hunt et al. 2009). An overview of the CALIOP science data processing architecture is provided in Winker et al. (2009).

The routine CALIOP lidar data processing includes two levels. In level 1 of data processing, the lidar backscatter data are geo-located and calibrated. The resulting altitude resolved profiles of attenuated backscatter coefficients are reported in the CALIOP level 1B data products (Hostetler et al. 2006; Vaughan et al. 2004). These level 1 profiles are further analyzed in level two, in order to derive the optical and physical properties of clouds and aerosols (Vaughan et al. 2004). The level two processing algorithms include three primary codes: First, the layer detection algorithm (SIBYL—Selective Iterated BoundarY Locator) finds the features (clouds, aerosols, surface, etc.) by searching for regions of enhanced signal in the attenuated backscatter profiles provided by the level 1 processing (Vaughan et al. 2009). After finding the features, mean values of the (532 and 1064) nm attenuated backscatter, attenuated total color ratio, and volume depolarization ratio were computed for each detected atmospheric feature (Rogers et al. 2011; Winker et al. 2013). These optical layer properties, along with the physical properties, such as top and base heights, latitude, and longitude, are reported in level two layer products. Based on these optical and physical properties, each atmospheric feature is then classified according to type by the Scene Classification Algorithm (SCA) (Liu et al. 2005). The lidar ratio (extinction-to-backscatter) is a key parameter, which is used in Hybrid Extinction Retrieval Algorithms (HERA) to retrieve particulate (aerosol or cloud) extinction and backscatter coefficients (Young and Vaughan 2009). The ratio does not depend on the number density of the particles, but rather on such physical and chemical properties as size distribution, and particle shape and composition (Liu et al. 2005).

NASA decided to split up the CALIPSO data into half orbit files, for day and night orbits, due to some problems, such as background noise in daytime (Vaughan et al. 2005). Then, after removing the same ancillary data, day and night data would be combined together as whole day data. At the end of processing, the final data products are extracted from these intermediate files. Table 1 lists the degree of averaging, which varies with altitude based on the mean sea level.

CALIPSO data products were generated in three standard data formats: (i) A Vertical Feature Mask (VFM) format, which provides information on the spatial and morphological distribution of features. (ii) A suite of cloud and aerosol layer products that provide statistical descriptions of all features detected. (iii) A set of profile product formats that map the vertical distributions of backscatter and extinction coefficients separately for both clouds and aerosols (Hostetler et al. 2006; Vaughan et al. 2006).

Table 1 The spatial resolutions for the CALIPSO on-board averaging scheme (adopted from Winker et al. 2006)

Altitude Region		Vertical resolution (m)	Horizontal resolution (m)	No. of profiles (per 5 km)	No. of samples for each profile
Base (km)	Top (km)				
30.1	40.0	300	5000	1	33
20.2	30.1	180	1667	3	55
8.2	20.2	60	1000	5	200
− 0.5	8.2	30	333	15	290
− 2.0	− 0.5	300	333	15	5

2.2 Generating a profile of mean CALIPSO aerosol extinction coefficient

We generated the vertical profiles of mean extinction coefficient and relative uncertainty from the CALIPSO level two profile products with data quality screening. The three profile descriptive flags (Atmospheric Volume Description (AVD), CAD score, and extinction QC) were applied to screen out the extinction coefficient samples, which have less confidence, as follows.

We used the level two aerosol profile granule. The extinction coefficient 532 nm and its uncertainty, and all the profile descriptive flag arrays (CAD score, AVD, and extinction QC flag) were used (Young and Vaughan 2009). The two arrays of extinction coefficient and its uncertainty indicate the number of altitudes and number of profiles, respectively; but applying the CALIPSO profile descriptive flags for quality screening is slightly ambiguous (Young and Vaughan 2009), due to the fact that they are stored in a three-array (index, the number of altitudes, and number of profiles). However, the first (index) is used to keep track of the two 30 m resolution layers in each 60 m extinction coefficient range bin (Young and Vaughan 2009). Afterwards, with an array of extinction coefficients, samples with less confidence were screened out (such as the information about clouds and stratospheric features), in order to identify bad profiles. Therefore, we kept the information about aerosols, which reflect the feature with majority that the scene classifier identifies for this region. We firstly screened out the fill values (CAD score of − 127), indicating that there are no samples to report. For the unscreened mean extinction coefficient, we simply filtered out all extinction coefficient samples that were not fill values. Then, for the screened mean extinction coefficient, we applied the three profile descriptive flags AVD, CAD score (eliminate features with CAD scores greater than − 20) (Young and Vaughan 2009), and extinction QC values (constrained to 0, or 1) to screen out extinction coefficient samples, and to preserve only the layers that have higher confidence to be identified as aerosols. In order to calculate the extinction coefficient 532 nm relative uncertainty, we divided the extinction coefficient uncertainty by the mean extinction coefficient (Young and Vaughan 2009), both with and without quality screening.

2.3 Discriminating aerosols

2.3.1 VFM data product analysis

The VFM data product is designed to provide scientists simple "where" and "what" information about any region within and along a track swath of the atmosphere (Vaughan et al. 2004). Furthermore, the VFM data product contains a one 16-bit integer, where each integer value includes a set of scene classification flags that characterize the corresponding spatial region in terms of feature presence and type (Vaughan et al. 2004). The descriptive information within these feature classification flags is described in detail in the PC-SCI-503 CALIPSO data products catalog (Version 3.3).

The aerosol discrimination algorithm distinguishes cloud scenes from aerosol scenes by interpreting the individual bits and the group of bits, which is provided in the PC-SCI-503 CALIPSO data products catalog (Version 3.3 Feature Classification Flag Definition Table). Meanwhile, the cloud-phase sub-algorithm used the interpretation of the feature-type bits (liquid and ice (bits 6 and 7)), as well as the cloud top and bottom temperatures. The cloud temperatures are calculated from the CALIOP-measured geometrical cloud heights, and the temperature-height relationship is obtained from the National Centers for Environmental Prediction–National Center for Atmospheric Research (NCEP–NCAR) reanalysis-2 data. In addition, six aerosol types were obtained from the surface type, depolarization ratio, mean attenuated backscatter, and CALIOP 5-km VFM (Versions 3.01 and 3.30). The aerosol phase in the

Table 2 The seasonal statistics of CALIOP aerosol distribution of Tabriz and Mashhad cities, Iran (2005–2016) (No.: The number of samples)

	Tabriz (%)				Mashhad (%)			
Season	No.	Min	Max	Mean	No	Min	Max	Mean
Spring	588	14.21	32.97	24.09	507	13.55	36.96	24.89
Summer	655	32.09	40.63	36.40	550	28.02	41.73	35.76
Fall	650	12.94	32.74	24.42	560	11.97	34.16	24.14
Winter	615	9.26	16.26	12.16	504	8.02	15.41	11.51

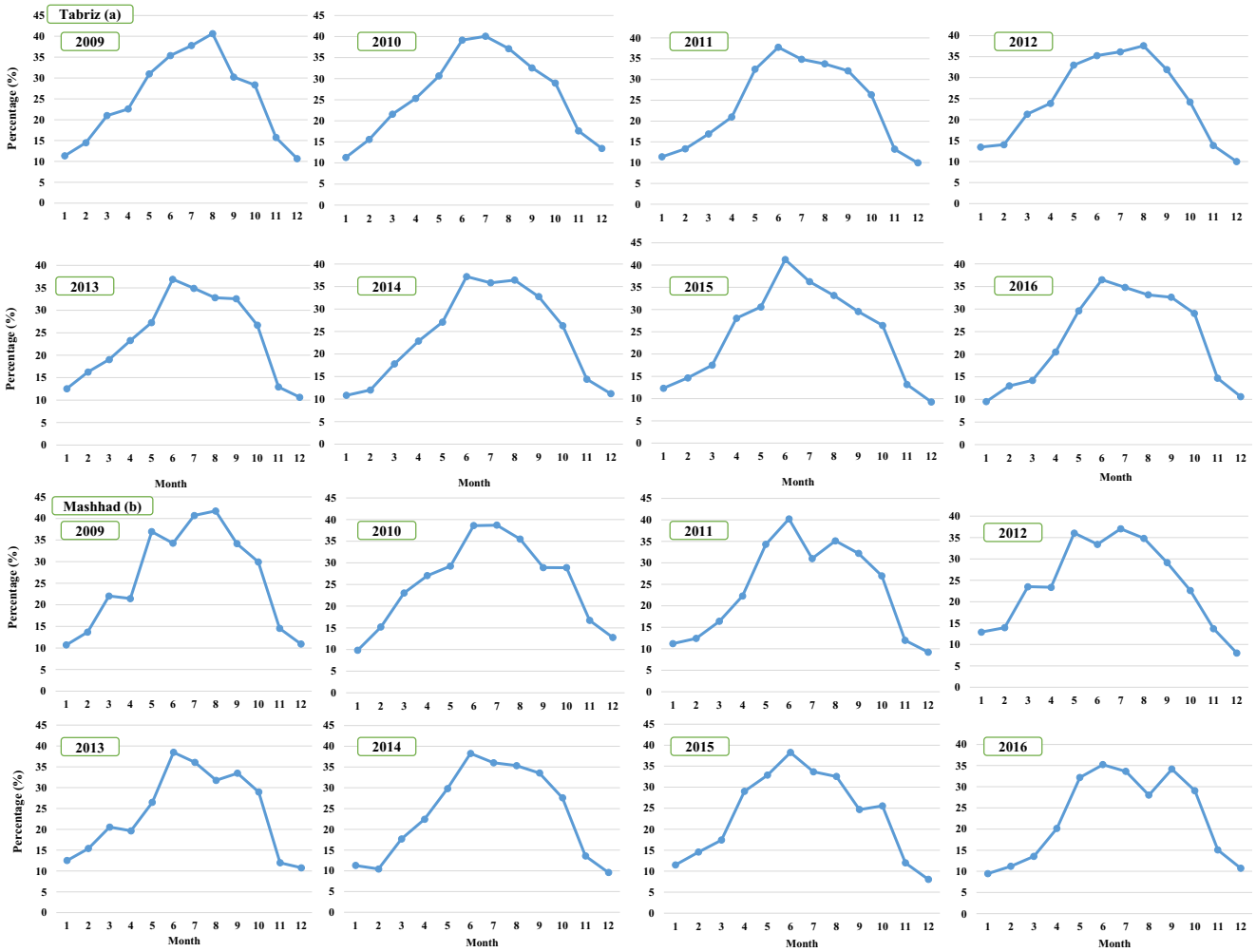

Fig. 2 Average monthly time series of CALIOP Aerosol Profile V4 (percentage) integrated from 0 to 8 km altitude of **a** Tabriz and **b** Mashhad, Iran, from 2009 to 2015

algorithm used the interpretation of the aerosol feature sub-type bits (six aerosol types (bits 10–12)), as well as the top and bottom heights of aerosol layer. As mentioned in Omar et al. (2002, 2004, 2006) and Burton et al. (2013), the aerosol types are desert dust, smoke from burning biomass, clean continental, polluted continental, marine, and polluted dust. These aerosols have different extinction-to-backscatter ratios (lidar ratios), and depend on factors such as size distribution, particle shape, and composition (Choi et al. 2010; Young and Vaughan 2009). In spite of the fact that this set does not cover all possible aerosol-mixing scenarios, especially for this region, it accounts for a majority of the meso-scale aerosol layers.

2.3.2 CALIOP aerosol profile product analysis

We analyzed the monthly time series of CALIOP Aerosol Profile V4 (Percentage) for (0 to 8) km altitude for different times, seasons and years, from 2005 to 2016, over Tabriz (Fig. 1c) and Mashhad (Fig. 1d) cities in the north-western and north-eastern regions of Iran. Table 2 summarizes the seasonal statistics of aerosol distribution.

Table 3 The CAD score distribution of CALIOP 5-km feature type, for August 2009 and July 2013 over Tabriz and Mashhad cities, Iran

CAD score		− 127	− 100 to − 20 aerosol (%)	− 20 to 20 no confidence (%)	20 to 100 cloud (%)	Special CAD scores (101,102, and 103)
Tabriz	2009/8	47.80	40.07	10.92	1.21	0
	2013/7	53.13	36.25	9.64	0.98	0
Mashhad	2009/8	45.32	42.75	11.13	0.80	0
	2013/7	51.65	39.89	8.24	0.22	0

Table 4 The CAD score distribution for different aerosol confidences on August 2009 and July 2013 over Tabriz and Mashhad cities, Iran

CAD score (%)	Tabriz		Mashhad	
	2009/8	2013/7	2009/8	2013/7
Not feature (NF*)	47.80	53.13	45.32	51.65
Aerosol high confidence	38.19	33.97	40.78	37.42
Aerosol medium confidence	1.16	1.45	1.25	1.64
Aerosol low confidence	0.72	0.83	0.68	0.84
No confidence	10.92	9.64	11.13	8.24
Cloud	1.21	0.98	0.80	0.22
101	0	0	0	0
102	0	0	0	0
103	0	0	0	0

*NF = − 127 (CAD score); aerosol high confidence = [− 100, − 70]; aerosol medium confidence = [− 70, − 50]; aerosol low confidence = [− 50, − 20]; no confidence = [− 20, 20]; cloud = [20, 100]; and 101, 102, and 103 are special CAD scores, respectively

The CALIOP aerosol distribution values show significant seasonal variability (Fig. 2). The values during summer are the highest ((40.63 and 41.73) %), while those in winter are the lowest ((9.25 and 8.02) %). Also, the largest mean value ((36.40 and 35.76) %) is in summer, while the lowest mean ((12.16 and 11.51) %) is in winter (for Tabriz and Mashhad, respectively).

According to the synoptic data records, these cities have high fraction of dust event occurrences and contamination load, based on the evidence recorded in the early summer of 2009 and 2013 (CRI 1996). The dust events, which affected many regions of Iran, could be seen in many city skies. Thus, we selected two summer months of August 2009 and July 2013 over the western and eastern parts of Iran.

The selected months for the region, due to their proximity and coincidence with religious and summer vacations for 2009 and 2013 (half of Sha'ban and Ramadan), as well as traffic load, have the same conditions for comparison. Figure 2 shows the average monthly time series of aerosol distribution (CALIOP Aerosol Profile V4) integrated for (0 to 8) km altitudes of north-western (Tabriz, Fig. 2a) and north eastern (Mashhad, Fig. 2b) parts of Iran for 2009 to 2016.

3 Assessment of CALIPSO data products over Iran

3.1 CAD score distribution

Table 3 presents the CAD score distribution of the CALIOP level two products in a percentile (integer) range of (−100 to 100) (positive: cloud and negative: aerosol) for the western and eastern parts of Iran.

The identification of features as clouds and aerosols was performed based on the values of the CAD score. A feature was classified as cloud when ($20 \leq CAD \leq 100$), as aerosol when $CAD \leq -20$, and no confidence (not cloud or aerosol) when $-20 < CAD < 20$ (Liu et al. 2009). The absolute value of the CAD score provides a confidence level for the feature classification that larger values of the CAD score, leading to an increase in the confidence of the classification. Also, the sign of the CAD score indicates layer type, so that clouds have positive CAD scores, while aerosols have negative CAD scores, along with the magnitude of the score indicating the degree of confidence in the classification (Liu et al. 2009; Winker et al. 2012).

Some features with CAD score values in the range of $|CAD| < 20$ cannot be identified with enough confidence, indicating no confidence. These feature layers may not be correctly measured, due to the detection issues, such as the detector transient response, two-way transmittance multiple scattering, and mixed layers of cloud and aerosol (Liu et al. 2009). Table 3 shows that we only classified the aerosol layers that had the magnitude of CAD scores between (100 and 20). The fraction of aerosols in August 2009 was more than that of July 2013. This is because of the stable flow of dust, internal dust sources (such as the Dasht-e Kavir and Lut Deserts), plus the dust flow that entered from the western neighbors of Iran in the summer of 2009. The Special CAD score of − 127 is actually unidentified, where the CALIOP algorithm has detected no feature. This could happen because the sample was of clear air, but it could also happen because the aerosol backscatters were below the layer detection threshold. Perfect interpretations of the special CAD scores (101, 102, and 103) are also reported in the CALIOP data product descriptions (Liu et al. 2009).

Table 4 presents the CAD score distribution for different aerosol confidences for western and eastern parts of Iran. The negative CAD values have been divided into high-confidence range ($70 \leq CAD \leq -100$), medium-confidence range ($-50 \leq CAD < -70$), and low-confidence range ($-20 \leq CAD < -50$), as a confidence level of the aerosol classification. The no-confidence range ($|CAD| \leq 20$), refers to the features that are neither classified as cloud, nor as aerosol (Fuchs and Cermak 2015; Liu et al. 2005, 2009). The number of features with the special score of 103, as a mixture of Horizontally Oriented Ice (HOI) and other types of cloud, is very low for these regions.

According to Table 4, the rate of aerosols with high-confidence range is more than the other ranges, since dust is the major aerosol subtype for these regions, which has the CAD score range from − 46 to − 100 based on our investigation. Additionally, prolongation of drought time and increasing desertification due to the increasing anthropogenic activities inside and outside of Iran will have a progressive impact on the process and the formation of dust storms. However, it is found that the aerosol pixel shows fair confidence, once it is identified as an aerosol, due to the aerosols in these regions

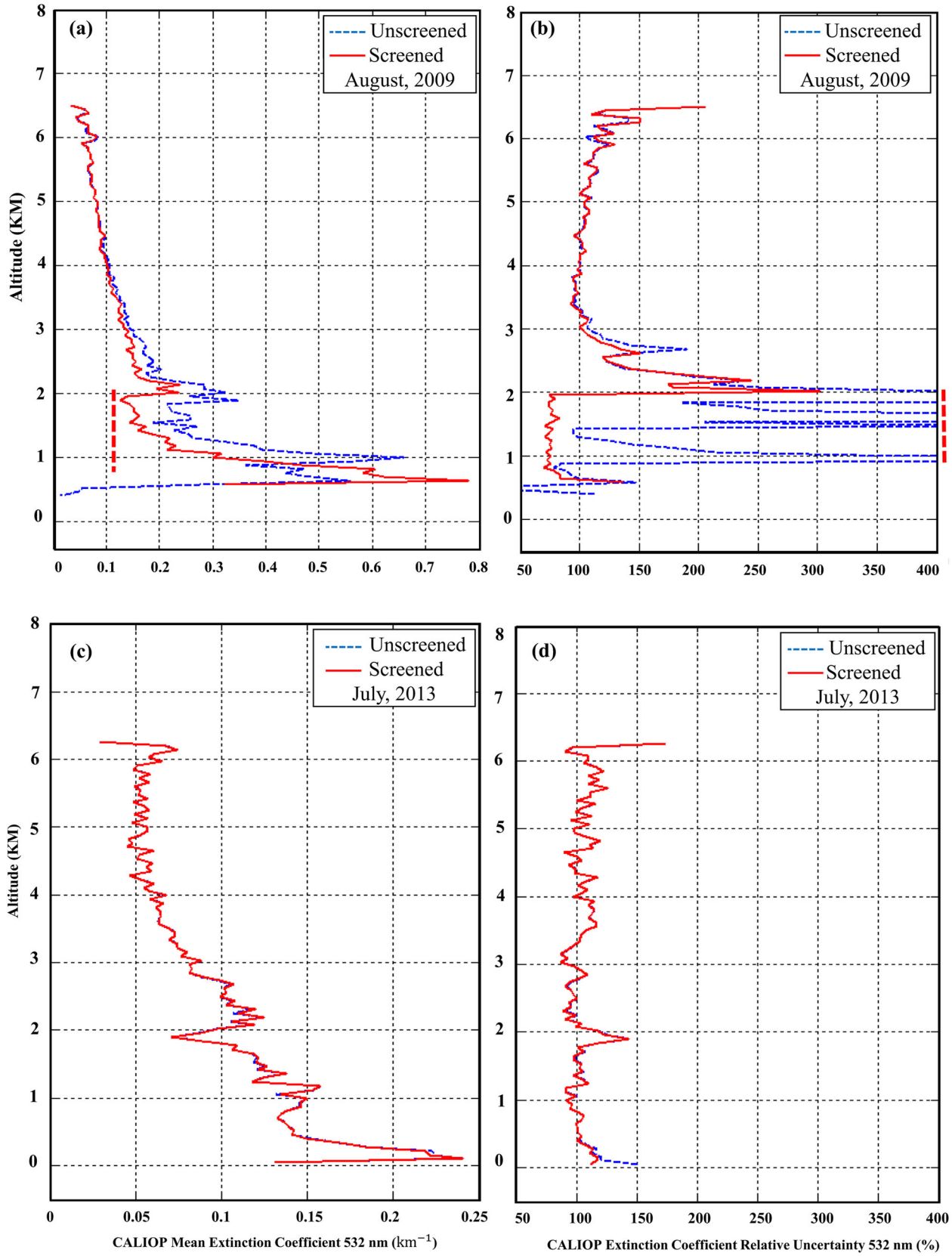

Fig. 3 **a**, **c** The mean extinction coefficient as a function of altitude, and **b**, **d** the relative extinction coefficient uncertainty in percent for the unscreened and screened cases over Iran on August 2009 and July 2013

Table 5 A preliminary assessment of the feature discrimination algorithm performance of expert manual classification of the CALIOP 5-km VFM over the Iran region, on August 2009 and July 2013

	Total features	No. of misclassified aerosols (%)		No. of misclassified clouds (%)		No. of no confidence (%)	
		2009/8	2013/7	2009/8	2013/7	2009/8	2013/7
Tabriz	1,307,000	3.98	0.06	0.98	4.02	2.78	0.05
Mashhad	1,286,900	4.27	0.04	0.82	3.54	2.01	0.04

being mostly dust, which finding is relatively more reliable than other types in the CALIOP algorithm. Thus, the future improvement of the algorithm should be to reduce Not Features (NFs), and identify more features.

3.2 Profiles of the mean CALIPSO aerosol extinction coefficient and its uncertainty

We generated a vertical profile of the CALIPSO mean aerosol extinction coefficient and the relative extinction coefficient uncertainty using the profile descriptive flags (included in CALIOP level two profile data product) for basic quality screening, in order to discriminate the aerosols over the investigated regions of Iran.

Figure 3 shows the mean extinction coefficient (Fig. 3a, c) and extinction coefficient relative uncertainty (Fig. 3b, d) profiles for the unscreened and screened cases over Iran in August 2009 and July 2013. The CALIPSO total attenuated backscatter measurements reveal an aerosol layer, which reflects the feature with majority measurement over the Iran region, extending from the northeast to the southeast. We applied the three-dimensional profile descriptive flags (AVD, CAD score, and extinction QC) to screen out the extinction coefficient samples of less confidence or no samples to report for this region. Moreover, the mean extinction coefficient was used to validate the adjustment of aerosols in CALIOP VFM data.

Based on Fig. 3a, the mean extinction coefficient below 2 km altitude tends to have high extinction coefficient values before screening. However, the majority of features that the scene classifier identified for this region are aerosol with low extinction coefficient values. In addition, its relative uncertainty below 2 km in Fig. 3b exceeded 400% before screening, but after removing a relatively small number of troublesome samples (CAD score of − 127, namely, troublesome samples or unidentified), it was reduced to a more manageable (70–140) % (Fig. 3b). The reason for having high extinction coefficient values, in particular below 2 km, could be the nature of a downward pointing lidar of having more uncertainty with decreasing altitude (Liu et al. 2005). Another reason is that the lidar level two identified clouds or some possible aerosol mixing types, such as mixed dust, biomass burning smoke, or lead pollution with high extinction coefficient values for low altitudes.

The mean extinction coefficient and its relative uncertainty were increased on August 2009 in comparison with July 2013 (Fig. 3), due to the increase of the extinction coefficient at 532 nm (Liu et al. 2009), and rise of the relative humidity on August 2009, considering that CALIOP could not penetrate the entire dense cloud layers due to the large attenuation of the clouds at the 532 nm wavelength. On the other hand, when CALIOP signals encounter dense cloud layers and/or thick aerosol plumes, the signal becomes attenuated towards the surface, and this is a known limitation of the CALIOP measurements (Liu et al. 2005; Nowottnick et al. 2011). This would be one of the reasons that the extinction coefficient was raised on August 2009, and the possibility that the cloud and thick aerosol's existence increased on this date. In addition, particulate concentrations vary dramatically depending on location, time of day, and time of year. More importantly, many particulates are hygroscopic, so the size and distribution of these particles are strongly dependent on the relative humidity (Kovalev and Eichinger 2004). Therefore, the rise of relative humidity on August 2009 compared to July 2013 caused the mean extinction coefficient and its relative uncertainty to increase.

3.3 Aerosol feature discrimination using CALIOP satellite data

We presented a preliminary assessment of the feature discrimination algorithm performance based on two critical summer months (August 2009 and July 2013) of expert manual classification of the CALIOP 5-km VFM, cloud, and aerosol layer datasets over the Iran region. Table 5 summarizes the assessment results based on these 2 months of CALIOP 5-km data (1,307,000 and 1,286,900 features for Tabriz and Mashhad,

Fig. 4 **a** The CALIOP ground track over Iran on July 28, 2013. **b** Attenuated backscatter measured by CALIOP at 532 nm in km^{-1} sr^{-1}, the color bar on the right indicates the value of total attenuated backscatter that assigned to ranges of attenuated backscatter. **c** The CALIOP depolarization ratio measurement. **d** The CALIOP vertical feature mask, feature types: 1, clear air; 2, cloud; 3, aerosol; 4, stratospheric layer; 5, surface; 6, subsurface; 7, no signal (total attenuated); and L, low/no confidence; and finally **e** the CALIOP aerosol subtype, feature sub-types: N/A, not applicable; 1, clean air; 2, dust; 3, polluted continental; 4, clean continental; 5, polluted dust; and 6, smoke. Meanwhile, the latitude and longitude based on "degrees." The black rectangle in these scenes depicts the east side of Iran

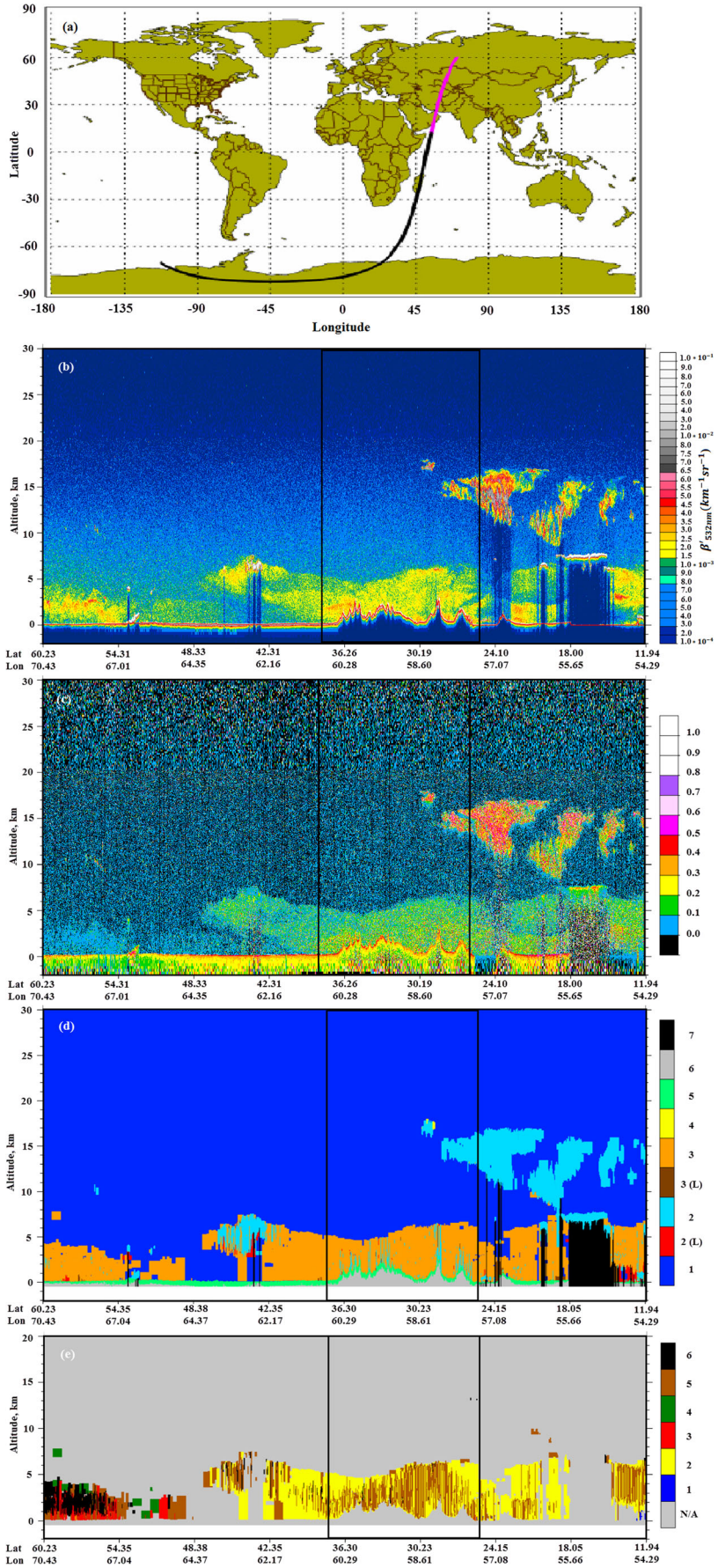
(a)
Latitude
Longitude
(b)
Altitude, km
(c)
(d)
(e)
Lat 60.23 54.31 48.33 42.31 36.26 30.19 24.10 18.00 11.94
Lon 70.43 67.01 64.35 62.16 60.28 58.60 57.07 55.65 54.29
Lat 60.23 54.35 48.38 42.35 36.30 30.23 24.15 18.05 11.94
Lon 70.43 67.04 64.37 62.17 60.29 58.61 57.08 55.66 54.29
N/A

respectively) and the measured meteorological data. We note that this assessment will not be representative of the whole CALIOP dataset, and it just provides a general idea about the performance of the feature discrimination algorithm for most regions of Iran.

In contrast to the cloud and aerosol feature and its sub-type discrimination computer code that performs feature classification in isolation (based on the properties of a single vertical layer), this expert manual reclassification identifies features by simultaneous investigations of two-dimensional vertical-horizontal images of a few different CALIOP measurements (CAD score, attenuated backscatter, attenuated backscatter color ratio, and volume depolarization ratio). We also make use of the additional information, such as the layer structures, geographic locations, connections with the surrounding layers, and textures in the expert manual classification of the feature types. For this purpose, a computer program has been developed to facilitate this type of image-based manual identification of features. The number of aerosols that were misclassified is less than clouds that were misclassified for July 2013, due to the mixed layers of cloud and aerosol at the edges of the clouds, and also the cloud layers below the dense aerosols, whose optical properties are not correctly estimated. Meanwhile, the percentage of aerosols, which were misclassified, is larger on August 2009. This happens due to the large fractions of the optically thin aerosols not being reliably detected during daytime scans due to detection issues, such as the detector transient response. Figure 4 provides an example of the aerosol feature and its sub-type classification over the east regions of Iran. The data were acquired by CALIOP on July 28 2013 from a nighttime orbit across northeast to southern Iran. Figure 4a shows the CALIOP ground track. Figure 4b, c presents the attenuated backscatter measured by CALIOP at 532 nm and the CALIOP depolarization ratio measurement, respectively (Rogers et al. 2011; Winker et al. 2013). Figure 4d, e shows the CALIOP vertical feature mask and the CALIOP aerosol subtype, respectively.

These scenes show a spatially extensive wind of 120 days, and dust layer of moderate optical thickness, which extends from ~40° N to the right hand side of the images at ~25° N. The winds, which are the major source of dust influencing Iran, are strong from mid-May to mid-September, when a persistent high-pressure system over the high mountains of the Hindu Kush in northern Afghanistan combines with a summertime thermal low over the desert lands of eastern Iran and western Afghanistan. This dust layer is easily identified from the depolarization ratio measurement (green-yellow colors in Fig. 4c). Meanwhile, dust aerosol can be well distinguished from the other aerosol types, based on checking of the volume depolarization ratio using a threshold of 0.06 (Liu et al. 2008). Vertically, this dust layer extends from the surface up to several kilometers (> 5 km for its highest part). Another aerosol subtype between (25 and 40)° N appears to be polluted dust (brownish color in Fig. 4e). The VFM image presented in Fig. 4d shows that the classification algorithm has identified some features correctly for this region. But several types of misclassifications have occurred with some frequency. These misclassifications or lesser identification might be due to the reduction of signal-to-noise ratio (SNR) during daytime, as a result of solar background illumination (Vaughan et al. 2005). Among these instances, the most prevalent are surface, cloud, and smoke aerosol. However, a few mixed layers of dust (blue strips between (25 and 37)° N in Fig. 4e) are correctly classified. Vertically, surface and subsurface layers (from the classification algorithm) between (25 and 36.5)° N extend from zero elevation up to a few kilometers (>2 km for its highest part). In addition, smoke, particularly over or near the source regions, is another aerosol type that can be misclassified, since the mean attenuated backscatter and mean attenuated total color ratio of this layer type are both relatively large. Thus, similar to what would be expected for cloud at the same altitude, this feature can be occasionally misclassified as cloud. The features colored in red, in depolarization ratio image (between (25 and 40)° N, from surface to 2 km in Fig. 4c) represent those features with large depolarization ratio (value of 0.5), comparable to those of dust particles (with value of 0.2). Finally, Fig. 5 shows the measured relative humidity and temperature profiles for the east part of Iran on July 28, 2013.

We used these measurements in order to validate and interpret the feature layers, which were associated with each other. So, four groups of measurements were used: (i) upper atmosphere (upper-air meteorological data), (ii) synoptic meteorological station datasets, provided by the East Azerbaijan and Khorasan Razavi Meteorological Organization, (iii) ground-based PM_{10} concentrations, acquired from the Department of Environment (DOE) of Tabriz and Mashhad, Iran, and (iv) AOD products of MODIS, obtained from the NASA Langley Research Center Atmospheric Science Data Center.

According to past studies, the behaviors of relative humidity and its inversion are certainly unknown yet, but the results indicate that humidity inversion near, and on top of cirrus cloud could happen (Nygård et al. 2014; Sedlar et al. 2012; Vihma et al. 2012). Furthermore, the probability of temperature inversion in cloudy condition is low, but the possibility of aerosol existence is increased. Figure 5a provides an example of observed relative humidity, and Fig. 5b shows temperature inversion below 5 km, as well as for the tropopause range ((10–20) km). Based on Fig. 5a, increasing mean relative humidity causes cloud formation below 5.0 km, which the CALIOP has also been able to detect the features as a cloud in the VFM product (Fig. 4d) for this range. The relatively strong temperature inversion layer below 5 km, which is shown in Fig. 5b, confined the aerosols to the region below this temperature inversion layer. Also, based on the VFM product (Fig. 4d), the conditions below 5 km of the temperature inversion layer (Fig. 5b) mean that this is the most appropriate level for aerosols and smoke formation.

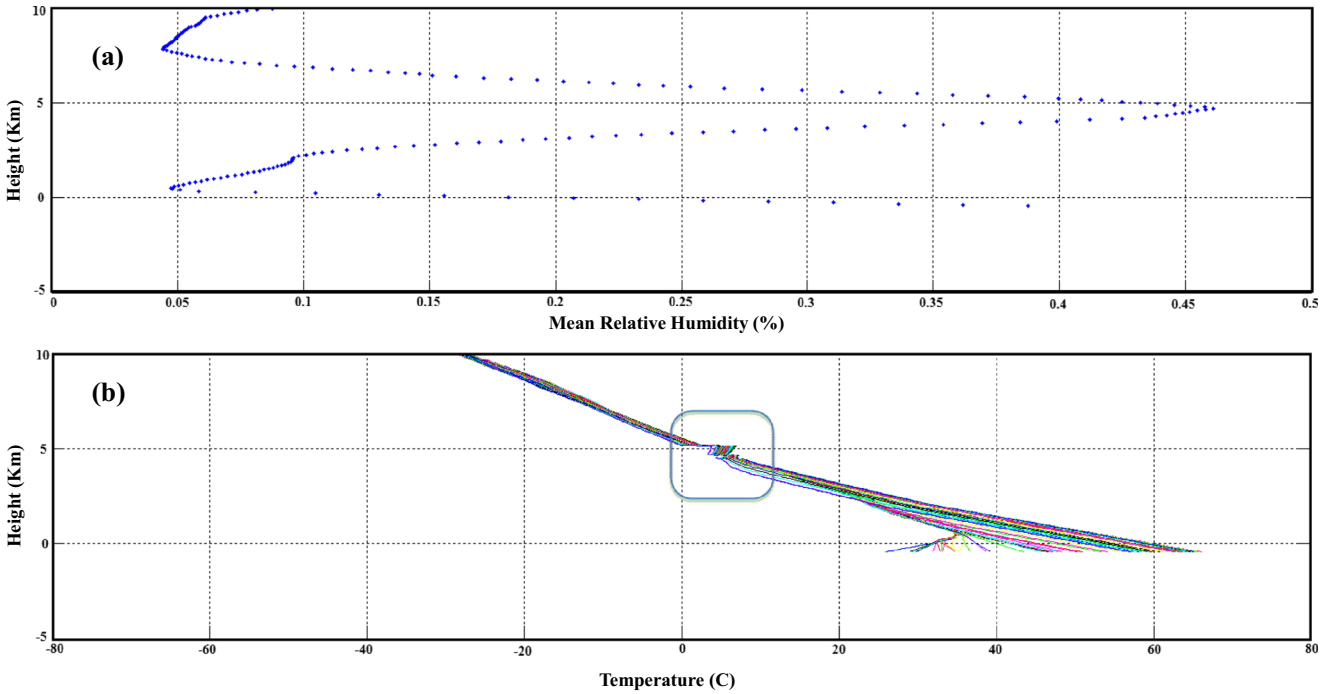

Fig. 5 The measured relative humidity and temperature profiles for the eastern part of Iran (from the Khorasan Razavi Meteorological Organization). **a** Mean relative humidity and **b** temperature profiles for July 28, 2013. The blue box in part (**b**) demonstrates the temperature inversion

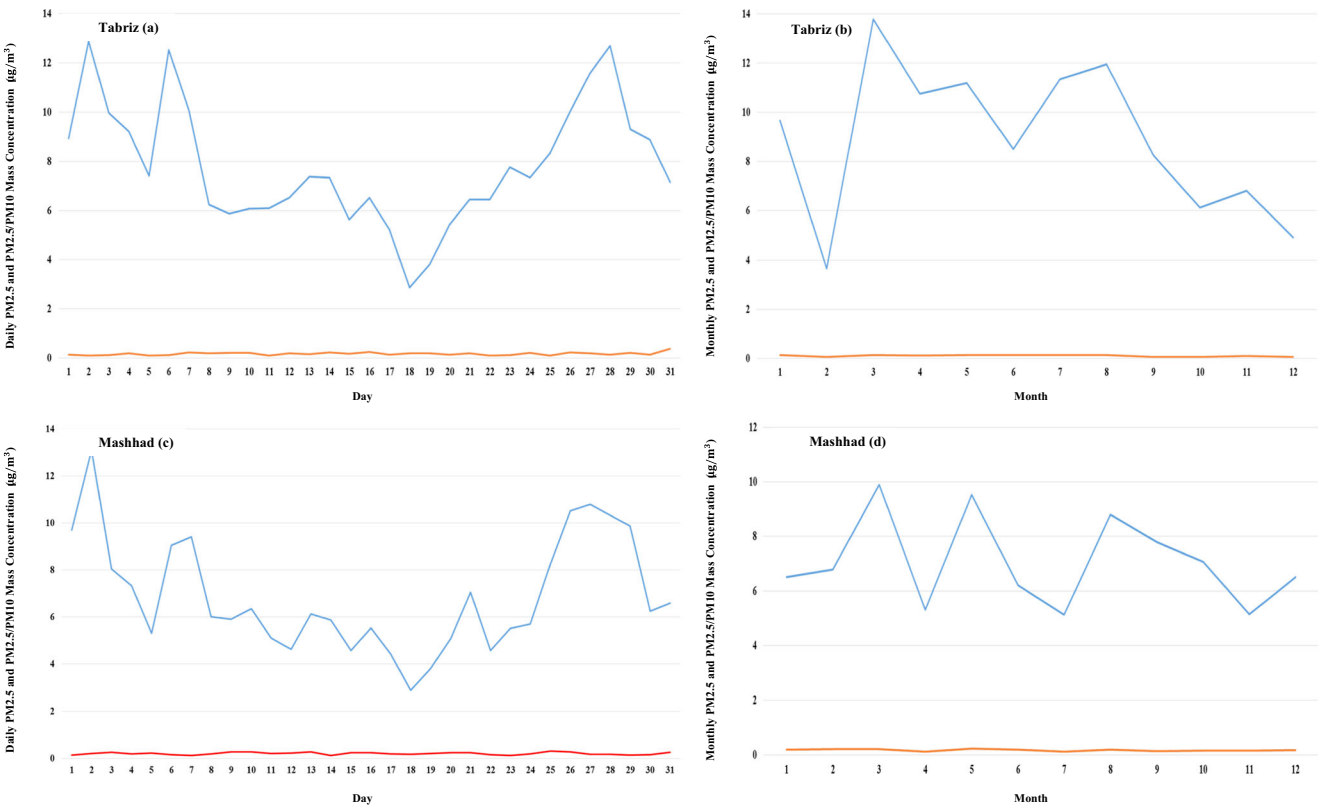

Fig. 6 Daily (**a**) and (**c**) ground level of $PM_{2.5}$ concentration (Blue) and $PM_{2.5}$ / PM_{10} (Red) on August 2011, and monthly (**b**) and (**d**) ground level of $PM_{2.5}$ concentration (Blue) and $PM_{2.5}$ / PM_{10} (Red) of Tabriz and Mashhad, Iran, for 2011

Table 6 The seasonal statistical of MODIS-AOD, MODIS-DBOD, and ground-level PM10 concentration (μg/m3) of Tabriz and Mashhad cities, Iran, from January 2005 to December 2014

Season		Tabriz				Mashhad			
		Min	Max	Mean	STD	Min	Max	Mean	STD
Spring	AOD	0.23	0.60	0.33	0.09	0.24	0.72	0.37	0.12
	DBOD	0.22	0.68	0.34	0.10	0.23	0.66	0.34	0.09
	PM_{10} ($\mu g/m^3$)	62.74	243.53	131.31	47.91	64.89	241.22	138.53	54.14
Summer	AOD	0.32	0.89	0.48	0.16	0.33	0.94	0.47	0.12
	DBOD	0.24	0.50	0.33	0.07	0.26	0.61	0.35	0.09
	PM_{10} ($\mu g/m^3$)	66.42	264.77	127.65	42.87	69.11	251.4	126.89	38.01
Fall	AOD	0.21	0.49	0.29	0.07	0.22	0.45	0.30	0.06
	DBOD	0.18	0.38	0.23	0.05	0.19	0.36	0.24	0.05
	PM_{10} ($\mu g/m^3$)	69.24	180.04	99.82	24.72	71.80	186.25	104.06	26.06
Winter	AOD	0.19	0.74	0.29	0.12	0.20	0.49	0.29	0.08
	DBOD	0.18	0.47	0.24	0.06	0.19	0.56	0.26	0.08
	PM_{10} ($\mu g/m^3$)	66.10	179.29	111.56	29.89	68.90	235.46	118.82	39.86

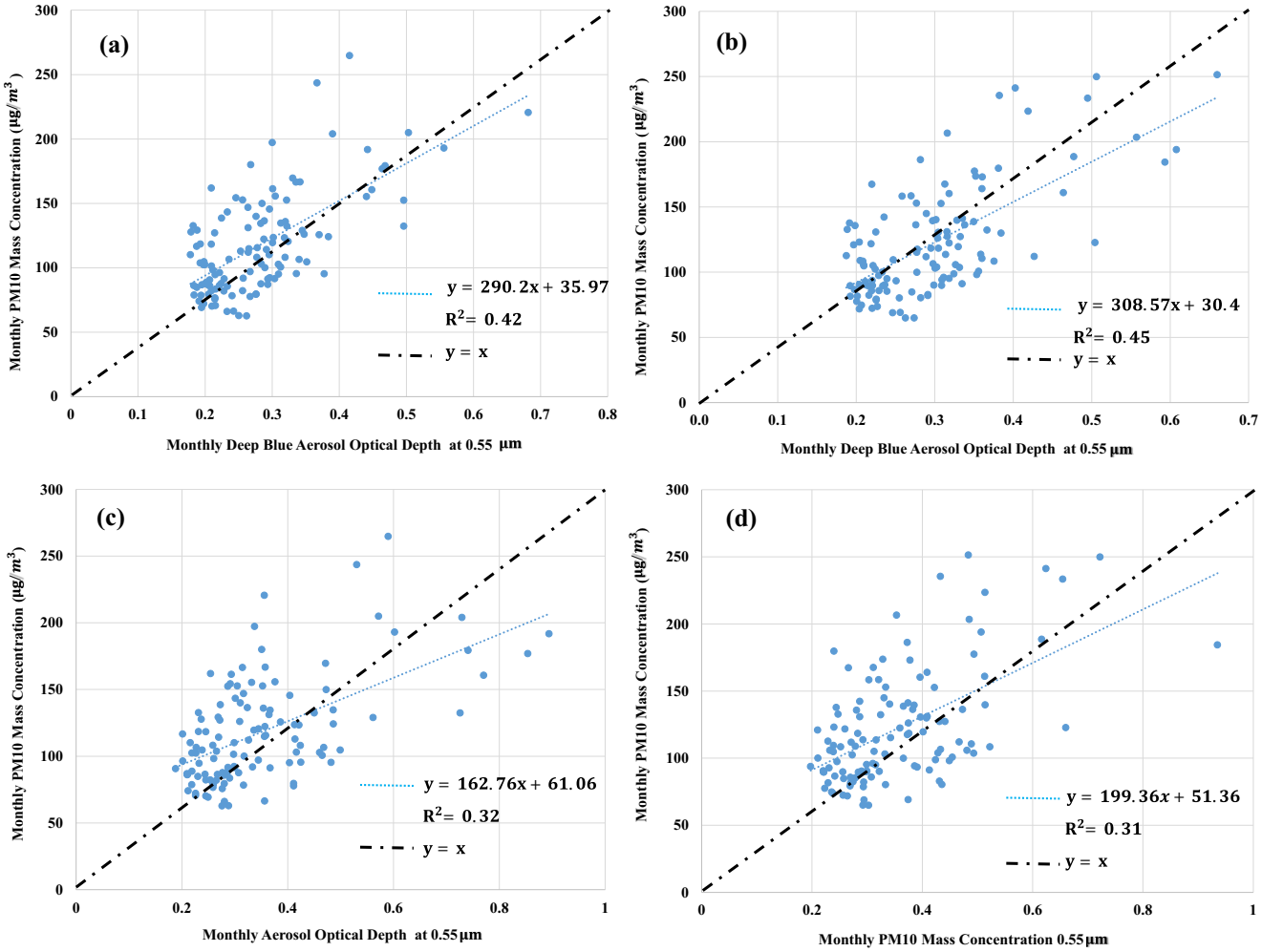

Fig. 7 The scatterplots of monthly ground-level PM_{10} concentration ($\mu g/m^3$) versus monthly MODIS Deep Blue Aerosol Optical Depth and monthly MODIS aerosol optical depth at 0.55 (μm) of (**a**) and (**c**) Tabriz, and (**b**) and (**d**) Mashhad, Iran, for 2005 to 2014

4 Statistical analysis of the seasonal MODIS-AOD, MODIS-DBOD, and ground-level PM_{10} concentration

The monthly-mean MODIS-AOD, MODIS-DBOD, ground-level PM_{10} concentration, and ground-based meteorological values for each air-quality monitoring station were calculated, using their daily values for years 2005 to 2016. Recent studies evaluated the Deep Blue algorithm and found it performs better than bright surfaces in terms of retrieval availability and $PM_{2.5}$ and PM_{10} estimations (Barladeanu et al. 2012; Geng et al. 2015; Seo et al. 2014; You et al. 2015, 2016; Zheng et al. 2013). Daily and monthly time-series of $PM_{2.5}$ and PM_{10} concentrations from 2005 to 2016 were analyzed. Figure 6 shows that in some periods of a season or a year, PM_{10} concentrations dominated over $PM_{2.5}$ concentrations. Thus, a ground level of PM_{10} concentration was used in the processing.

We used 3652 and 3593 datasets from 2005 to 2014 for modeling, and 731,719 datasets from 2015 to 2016 for the validation of statistical models according to stations that measured the PM_{10} data in Tabriz and Mashhad, respectively. Note that the monthly-mean values were only used for validation, and also data with the number of daily samples in a month less than five per monitoring station were excluded. Table 6 that shows the significant seasonal variability summarizes the seasonal statistics of PM_{10} mass concentration, MODIS AOD, and DBOD.

The MODIS AOD values during summer were the highest and had the lowest values in winter, and also MODIS DBOD values showed the highest and lowest values in spring and fall, respectively (Table 6). However, for the PM_{10} mass concentration, the largest monthly mean value was in summer of 2009, and the lowest monthly mean was in spring of 2005. The mean PM_{10} mass concentrations in spring and summer were almost the same. To illustrate the relation between the MODIS AOD and MODIS DBOD values with ground-level PM_{10} concentration, we developed a simple linear regression model between the MODIS-derived AOD and ground-level PM_{10} concentration for both Tabriz and Mashhad cities, Iran. Figure 7 shows the scatterplots of monthly ground-level PM_{10} concentration versus MODIS AOD and MODIS DBOD at 0.55 (μm) for Tabriz and Mashhad cities, Iran on 2005 to 2014.

The R^2 value between the monthly ground-level PM_{10} concentration and monthly MODIS DBOD is more correlated than the monthly MODIS AOD. Figure 7 clearly shows a relatively good relationship between ground-level PM_{10} concentration and MODIS DBOD for both cities. Accordingly, the simple linear regression model of MODIS DBOD and ground-level PM_{10} were implemented to estimate PM_{10} concentrations for 2015 to 2016. Table 7 provides the validation of the linear regression model of estimated monthly PM_{10} concentration ($\mu g/m^3$) based on the monthly DBOD at five independent air-quality monitoring stations of Tabriz and Mashhad, Iran from 2015 to 2016.

5 Summary and future work

In this study, we examined a vertical profile of CALIPSO mean aerosol extinction coefficient, the relative extinction coefficient uncertainty using profile descriptive flags included in the CALIOP level two profile data products for basic quality screening and MODIS Deep Blue Aerosol Optical Depth (DBOD) at wavelengths of 0.55 μm. The ground-based PM_{10} measurements were analyzed and evaluated for different times, seasons and years, from 2005 to 2016, over Tabriz and Mashhad cities in the north-western and north-eastern regions of Iran.

We investigated the profiles of the particle backscatter and extinction coefficient, as well as information on the determined feature type (e.g., clouds or aerosols) and aerosol subtype (e.g., dust, and smoke) from the VFM data product on two crucial months of August 2009 and July 2013 that were statistically selected from 2009 to 2016. The cloud and aerosol discrimination algorithm and the VFM data product work properly for some feature types, but several specific layer types are still misclassified. Among these, the most prevalent are cloud and smoke layer types, which are misclassified with less frequency. Meanwhile, the clouds that can extend from the surface to several kilometers in altitude are misclassified as aerosol. However, smoke layers are misclassified as cloud less frequently than dust layers are. The evaluation of comparison of the relative humidity, temperature, and their inversion shows that the performance of the CALIOP in the detection

Table 7 Validation of the linear regression model of the seasonal statistical of MODIS-DBOD and ground-level PM10 concentration (μg/m3) of Tabriz and Mashhad cities, Iran, from 2015 to 2016 (No.: The number of samples)

	Tabriz				Mashhad			
Season	Spring	Summer	Fall	Winter	Spring	Summer	Fall	Winter
No.	731				719			
RMSE (%)	21.63	20.61	23.59	30.25	18.96	22.65	17.47	23.24

of aerosols in mid-troposphere (around 5.0 km) is better than in cloud detection.

Additionally, the correlations of the PM_{10} concentration, MODIS AOD, and MODIS DBOD were investigated for January 2005 to December 2014. The overall correlation analysis shows that monthly ground-based PM_{10} concentration measurements have good correlation (r = (0.65 and 0.67) for Tabriz and Mashhad, respectively) with monthly MODIS DBOD than MODIS AOD for different seasons.

Differences in investigation of the CALIPSO dataset with the actual measured values show that some modifications of the relative humidity, temperature and its inversion (instead of satellite measurements), MODIS DBOD, and ground-based PM_{10} concentration should be made, and also considered in the cloud and aerosol discrimination algorithm for this region. Therefore, in the future study, combining field measurements, including relative humidity, temperature and its inversion, with CALIOP data will be necessary. More importantly, the vertical aerosol type distributions should be further partitioned according to geographic region, day vs. night, and season. Finally, an attempt to optimize the use of CALIOP data and improve the results, which is combined with other meteorological and A-Train data, would be the objectives of subsequent studies.

Acknowledgments We wish to acknowledge the staff at the Center for Climate/Environment Change Prediction Research for their help in improving this work, and the NASA Langley Research Center Atmospheric Science Data Center for providing the CALIPSO and MODIS products. In addition, we wish to thank East Azerbaijan, Khorasan Razavi Meteorological Organization, and the Department of Environment (DOE) of Tabriz and Mashhad, Iran, for their great help in supplying the synoptic meteorological station datasets and ground-based PM_{10} and $PM_{2.5}$ concentrations to conduct this study, without any financial expectation.

Funding information This research was supported by Basic Science Research Program through the National Research Foundation of Korea (NRF) funded by the Ministry of Education (2018R1A6A1A08025520).

References

Barladeanu R, Stefan S, Radulescu R (2012) Correlation between the particulate matter (PM10) mass concentrations and aerosol optical depth in Bucharest, Romania. Rom Rep Phys 64:1085–1096

Burton S, Ferrare R, Vaughan M, Omar A, Rogers R, Hostetler C, Hair J (2013) Aerosol classification from airborne HSRL and comparisons with the CALIPSO vertical feature mask. Atmos Meas Tech 6: 1397–1412

Cao H, Amiraslani F, Liu J, Zhou N (2015) Identification of dust storm source areas in West Asia using multiple environmental datasets. Sci Total Environ 502:224–235

Chan MA, Comiso JC (2011) Cloud features detected by MODIS but not by CloudSat and CALIOP. Geophys Res Lett 38

Chand D, Anderson T, Wood R, Charlson R, Hu Y, Liu Z, Vaughan M (2008) Quantifying above-cloud aerosol using spaceborne lidar for improved understanding of cloudy-sky direct climate forcing. J Geophys Res Atmos (1984–2012) 113

Choi YS, Park RJ, Ho CH (2009) Estimates of ground-level aerosol mass concentrations using a chemical transport model with moderate resolution imaging spectroradiometer (MODIS) aerosol observations over East Asia. J Geophys Res Atmos (1984–2012) 114

Choi Y-S, Lindzen RS, Ho C-H, Kim J (2010) Space observations of cold-cloud phase change. Proc Natl Acad Sci 107:11211–11216

CRI (1996) The Climatological Research Institute (CRI)

Duncan BN, Prados AI, Lamsal LN, Liu Y, Streets DG, Gupta P, Hilsenrath E, Kahn RA, Nielsen JE, Beyersdorf AJ (2014) Satellite data of atmospheric pollution for US air quality applications: examples of applications, summary of data end-user resources, answers to FAQs, and common mistakes to avoid. Atmos Environ 94:647–662

Emili E, Popp C, Petitta M, Riffler M, Wunderle S, Zebisch M (2010) PM10 remote sensing from geostationary SEVIRI and polar-orbiting MODIS sensors over the complex terrain of the European alpine region. Remote Sens Environ 114:2485–2499

Escribano J, Gallardo L, Rondanelli R, Choi Y-S (2014) Satellite retrievals of aerosol optical depth over a subtropical urban area: the role of stratification and surface reflectance. Aerosol Air Qual Res 14:596–568

Fuchs J, Cermak J (2015) Where aerosols become clouds—potential for global analysis based on CALIPSO data. Remote Sens 7:4178–4190

Geng G, Zhang Q, Martin RV, van Donkelaar A, Huo H, Che H, Lin J, He K (2015) Estimating long-term PM 2.5 concentrations in China using satellite-based aerosol optical depth and a chemical transport model. Remote Sens Environ 166:262–270

Gupta P, Christopher SA (2008) An evaluation of Terra-MODIS sampling for monthly and annual particulate matter air quality assessment over the southeastern United States. Atmos Environ 42:6465–6471

Hostetler CA, Liu Z, Reagan J, Vaughan M, Winker D, Osborn M, Hunt W, Powell K, Trepte C (2006) CALIOP algorithm theoretical basis document: calibration and level 1 data products. Doc PC-SCI 201

Hunt WH, Winker DM, Vaughan MA, Powell KA, Lucker PL, Weimer C (2009) CALIPSO lidar description and performance assessment. J Atmos Ocean Technol 26:1214–1228

Kovalev VA, Eichinger WE (2004) Elastic lidar: theory, practice, and analysis methods. John Wiley & Sons

Laity JJ (2009) Deserts and desert environments. John Wiley & Sons

Lee HJ, Chatfield RB, Strawa AW (2016) Enhancing the applicability of satellite remote sensing for PM2. 5 estimation using MODIS deep blue AOD and land use regression in California, United States. Environ Sci Technol 50:6546–6555

Lei H, Wang J (2014) Observed characteristics of dust storm events over the western United States using meteorological, satellite, and air quality measurements. Atmos Chem Phys 14:7847–7857

Liu Z, Omar A, Hu Y, Vaughan M, Winker D, Poole L, Kovacs T (2005) CALIOP algorithm theoretical basis document, part 3: scene classification algorithms. NASA-CNES document PC-SCI-203

Liu Y, Franklin M, Kahn R, Koutrakis P (2007) Using aerosol optical thickness to predict ground-level PM 2.5 concentrations in the St. Louis area: a comparison between MISR and MODIS. Remote Sens Environ 107:33–44

Liu D, Wang Z, Liu Z, Winker D, Trepte C (2008) A height resolved global view of dust aerosols from the first year CALIPSO lidar measurements. J Geophys Res Atmos (1984–2012) 113

Liu Z, Vaughan M, Winker D, Kittaka C, Getzewich B, Kuehn R, Omar A, Powell K, Trepte C, Hostetler C (2009) The CALIPSO lidar cloud and aerosol discrimination: version 2 algorithm and initial assessment of performance. J Atmos Ocean Technol 26:1198–1213

Mei L, Xue Y, Guang J, Li Y, Wan Y, Bai L, Ai J (2009) Aerosol optical depth retrieval over land using MODIS data and its application in monitoring air quality. Geoscience and Remote Sensing Symposium, 2009 IEEE International, IGARSS 2009. IEEE, pp V-421–V-424

Nowottnick E, Colarco P, da Silva A, Hlavka D, McGill M (2011) The fate of Saharan dust across the Atlantic and implications for a central American dust barrier

Nygård T, Valkonen T, Vihma T (2014) Characteristics of Arctic low-tropospheric humidity inversions based on radio soundings. Atmos Chem Phys 14:1959–1971

Omar AH, Won J-G, Yoon S-C, McCormick MP (2002) Estimation of aerosol extinction-to-backscatter ratios using AERONET measurements and cluster analysis. Lidar remote sensing in atmospheric and earth sciences: reviewed and revised papers presented at the 21st International Laser Radar Conference (ILRC). Quebec, Canada, pp 373–376

Omar AH, Winker DM, Won J-G (2004) Aerosol models for the CALIPSO lidar inversion algorithms Remote Sensing. International Society for Optics and Photonics, pp 153–164

Omar AH, Winker DM, Vaughan MA (2006) Selection algorithm for the CALIPSO lidar aerosol extinction-to-backscatter ratio. Remote sensing. International Society for Optics and Photonics, pp 63670M–63670M-63610

Rogers RR, Hostetler CA, Hair JW, Ferrare RA, Liu Z, Obland MD, Harper DB, Cook AL, Powell KA, Vaughan MA (2011) Assessment of the CALIPSO Lidar 532 nm attenuated backscatter calibration using the NASA LaRC airborne high spectral resolution lidar. Atmos Chem Phys 11:1295–1311

Sedlar J, Shupe MD, Tjernström M (2012) On the relationship between thermodynamic structure and cloud top, and its climate significance in the Arctic. J Clim 25:2374–2393

Seo S, Kim J, Lee H, Jeong U, Kim W, Holben B, Kim S, Song C, Lim J (2014) Spatio-temporal variations in PM10 concentrations over Seoul estimated using multiple empirical models together with AERONET and MODIS data collected during the DRAGON-Asia campaign. Atmos Chem Phys Discuss 14:21709–21748

Song C-K, Ho C-H, Park RJ, Choi Y-S, Kim J, Gong D-Y, Lee Y-B (2009) Spatial and seasonal variations of surface PM10 concentration and MODIS aerosol optical depth over China. Asia-Pac J Atmos Sci 45:33–43

Tian J, Chen D (2010a) A semi-empirical model for predicting hourly ground-level fine particulate matter (PM 2.5) concentration in southern Ontario from satellite remote sensing and ground-based meteorological measurements. Remote Sens Environ 114:221–229

Tian J, Chen D (2010b) Spectral, spatial, and temporal sensitivity of correlating MODIS aerosol optical depth with ground-based fine particulate matter (PM2. 5) across southern Ontario. Can J Remote Sens 36:119–128

Van Donkelaar A, Martin RV, Park RJ (2006) Estimating ground-level PM2. 5 using aerosol optical depth determined from satellite remote sensing. J Geophys Res Atmos 111

Van Donkelaar A, Martin RV, Levy RC, da Silva AM, Krzyzanowski M, Chubarova NE, Semutnikova E, Cohen AJ (2011) Satellite-based estimates of ground-level fine particulate matter during extreme events: a case study of the Moscow fires in 2010. Atmos Environ 45:6225–6232

Vaughan MA, Young SA, Winker DM, Powell KA, Omar AH, Liu Z, Hu Y, Hostetler CA (2004) Fully automated analysis of space-based lidar data: an overview of the CALIPSO retrieval algorithms and data products. Remote Sensing. International Society for Optics and Photonics, pp 16–30

Vaughan M, Winker D, Powell K (2005) CALIOP Algorithm Theoretical Basis Document, part 2: Feature detection and layer properties algorithms, PC-SCI-202.01, NASA Langley Res. Cent., Hampton, Va

Vaughan M, Winker D, Powell K (2006) CALIOP Algorithm Theoretical Basis Document–Part 2: Feature detection and layer properties algorithms Release 1.01. PC-SCI-202 Part 2, NASA Langley Research Center, Hampton, Virginia, USA, available at: http://www-calipso.larc.nasa.gov/resources/project_documentation.php. Last access: 10 June 2010

Vaughan MA, Powell KA, Winker DM, Hostetler CA, Kuehn RE, Hunt WH, Getzewich BJ, Young SA, Liu Z, McGill MJ (2009) Fully automated detection of cloud and aerosol layers in the CALIPSO lidar measurements. J Atmos Ocean Technol 26:2034–2050

Vihma T, Kilpeläinen T, Manninen M, Sjöblom A, Jakobson E, Palo T, Jaagus J, Maturilli M (2012) Characteristics of temperature and humidity inversions and low-level jets over Svalbard fjords in spring. Adv Meteorol 2011

Winker DM, Hostetler CA, Vaughan MA, Omar AH (2006) CALIOP algorithm theoretical basis document, part 1: CALIOP instrument, and algorithms overview. Release 2:29

Winker DM, Vaughan MA, Omar A, Hu Y, Powell KA, Liu Z, Hunt WH, Young SA (2009) Overview of the CALIPSO mission and CALIOP data processing algorithms. J Atmos Ocean Technol 26:2310–2323

Winker D, Pelon J, Coakley J Jr, Ackerman S, Charlson R, Colarco P, Flamant P, Fu Q, Hoff R, Kittaka C (2010) The CALIPSO mission: A global 3D view of aerosols and clouds

Winker D, Tackett J, Getzewich B, Liu Z, Vaughan M, Rogers R (2012) The global 3-D distribution of tropospheric aerosols as characterized by CALIOP. Atmos Chem Phys Discuss 12:24847–24893

Winker D, Tackett J, Getzewich B, Liu Z, Vaughan M, Rogers R (2013) The global 3-D distribution of tropospheric aerosols as characterized by CALIOP. Atmos Chem Phys 13:3345–3361

Yap X, Hashim M (2013) A robust calibration approach for PM10 prediction from MODIS aerosol optical depth. Atmos Chem Phys 13:3517–3526

You W, Zang Z, Zhang L, Li Z, Chen D, Zhang G (2015) Estimating ground-level PM10 concentration in northwestern China using geographically weighted regression based on satellite AOD combined with CALIPSO and MODIS fire count. Remote Sens Environ 168:276–285

You W, Zang Z, Zhang L, Zhang M, Pan X, Li Y (2016) A nonlinear model for estimating ground-level PM 10 concentration in Xi'an using MODIS aerosol optical depth retrieval. Atmos Res 168:169–179

Young SA, Vaughan MA (2009) The retrieval of profiles of particulate extinction from cloud-aerosol lidar infrared pathfinder satellite observations (CALIPSO) data: algorithm description. J Atmos Ocean Technol 26:1105–1119

Yu H, Zhang Y, Chin M, Liu Z, Omar A, Remer LA, Yang Y, Yuan T, Zhang J (2012) An integrated analysis of aerosol above clouds from A-train multi-sensor measurements. Remote Sens Environ 121:125–131

Zheng J, Che W, Zheng Z, Chen L, Zhong L (2013) Analysis of spatial and temporal variability of PM10 concentrations using MODIS aerosol optical thickness in the Pearl River Delta region, China. Aerosol Air Qual Res 13:862–876

Zieger P, Weingartner E, Henzing J, Moerman M, Leeuw GD, Mikkilä J, Ehn M, Petäjä T, Clémer K, Roozendael MV (2011) Comparison of ambient aerosol extinction coefficients obtained from in-situ, MAX-DOAS and LIDAR measurements at Cabauw. Atmos Chem Phys 11:2603–2624